



International Journal of Innovative Research in Science Engineering and Technology (IJIRSET)

(A Monthly, Peer Reviewed, Refereed, Scholarly Indexed, Open Access Journal)



Impact Factor: 8.699

Volume 15, Issue 2, February 2026

Modeling Heterogeneous Particle Size Distribution and Compression Index Influence on Uneven Settlement in Peat Soil

Amadi. P.N, Oba A. L, Eluozo S.N.

Department of Civil Engineering, Faculty of Engineering, River State University, Nigeria

amadi.ndidi@ust.edu.ng, achemie.oba@ust.edu.ng, solomon.eluozo@ust.edu.ng

ABSTRACT: The heterogeneous settling of peat soil poses a major problem in geotechnical engineering because of its composition and high-water content, which is not matched by any other soil type. The inhomogeneity in particle sizes in peat soil results in different levels of compressibility. There are no systematic simulation models in ongoing studies that consider the complicated relationship between the size distribution of particles and the compression index in peat soils, especially regarding their effect on uneven settlement. This paper seeks to create an accurate simulation model for forecasting the uneven settlement in peat soil through comparisons between predicted and experimental values. The goals are to determine the validity of the model, its sensitivity characteristics to compression indices, and valid ranges for critical geotechnical components. Measurements taken at various levels and time spans provided information regarding the settlement that occurred. This included geotechnical investigations, groundwater observation, and instrument placement to observe the vertical movement resulting in settlement. To simulate the irregular settlement of peat soil, there was development of a mathematical model was developed. The mathematical model has relevant input variables such as particle size distribution and compression index; the predicted models of these variables are validated through experimentation. Permissible Limits: The research sets acceptable levels of important factors that affect settlement. These include that the compression index, or C_c , should be kept below 0.6, although the best particle size distribution is between 30% and 50% finer particles. The void ratio should range between 2.0 and 5.0, while total settlements should not exceed 25-50 mm for normal situations, and 10-20 mm for critical situations. The outcome indicates a clear relationship between the values derived from the simulation and the data obtained from the experiment, especially in the settlement rate in terms of time and depth. The model demonstrates well how higher values of compressibility and particle size variability are critical in inducing heterogeneous settlement rates. This study is an advancement in the understanding of the behavior of peat soil, as it provides an accurate simulation model to help in the application of engineering in peat environments. This study also helps in recognizing hazardous regions of uneven distribution while setting permissible limits. The developed simulation model has made a significant improvement in the determination of irregular settlement in peat soil. Future studies will be oriented towards improving the parameters of the model as well as increasing the data gathered on-site in order to make the model more accurate and reliable. Guidelines will help in designing safe engineering structures in areas with peat soil.

KEYWORDS: Modeling, Particle Size Distribution, Compression Index, Uneven Settlement, and Peat Soil

I. INTRODUCTION

Peat soil has a heterogeneous particle size distribution due to its composition of organic matter and high-water content. It generally consists of a diverse assortment of particle sizes, including fibres, roots, and decomposed plant matter. Heterogeneous particle size distribution in soil indicates the presence of particles of different sizes dispersed across its whole. Peat soil with a varied range of particle sizes might experience uneven settling as a result of the differential compression of these distinct particle sizes. Smaller particles, such as small fibres and organic materials, exhibit greater compressibility compared to bigger particles, such as roots or woody debris. Consequently, in the process of consolidation, the smaller particles may undergo faster and extensive compression compared to the bigger particles. The differential compression results in uneven settlement, with regions with a greater concentration of smaller particles experiencing more settling compared to regions with bigger particles. Non-uniform settlement may lead to differential ground movements, which can create unevenness and possible structural issues in structures or infrastructure built on

peat soil. The compression index, often known as C_c , is a geotechnical measure used to quantify the compressibility of a soil. The consolidation coefficient is obtained via consolidation tests and corresponds to the gradient of the compression curve when plotted on a semilogarithmic scale. The compression index quantifies the degree to which a soil consolidates in response to a certain increase in effective stress. The compression index of peat soil indicates the degree of compressibility of the organic matter it contains. More compression index values imply more compressibility, indicating that the soil experiences more settling for a given increase in stress. Peat soil with a high compression index is prone to experiencing substantial settling during the consolidation process. The settlement might worsen if the compression index changes spatially within the soil mass. Regions characterised by higher compression index values will undergo more settlement in comparison to regions with lower compression index values. Hence, peat soil with a high compression index will result in uneven settling, since distinct regions of the soil would undergo varying degrees of compression. Differential settling and associated structural difficulties may arise because of this uneven compression. The uneven settling is influenced by both the heterogeneous particle size distribution and the compression index of peat soil. Differential compression occurs due to the existence of particles of varying sizes, resulting in greater settling of smaller particles compared to bigger ones. Furthermore, a high compression index signifies a greater degree of compressibility and an elevated likelihood of settlement. Hence, the convergence of these forces might result in irregular distribution patterns in peat soil settling.

Cemented paste backfill (CPB) is an emerging environmentally-friendly substance used in green mining. It consists of waste rocks, cementing ingredients, and water [1-3]. The primary function of this system is to regulate the movement of layers and the sinking of the surface, therefore minimizing the wastage of land resources and the contamination of water resources resulting from waste rock and tailings in the mining area [4-7]. Hence, CPB technology yields substantial economic, environmental, and safety advantages. The structure of CPB typically experiences compressive forces during its entire lifespan. It is important to examine the strength of the backfill during compression in order to ensure its mechanical stability [8-10]. Many studies have examined the strength properties of CPB, primarily by investigating variations in cementing materials (including type and content), additives (such as nano-materials, polymers, fibres, alkaline substances, and water-absorbing substances), and environmental factors (such as temperature, corrosion, and conservation). According to our understanding, CPB is a kind of porous material made up of waste rock particles (also known as tailings), substances that bind the particles together (such as cementing ingredients), and empty spaces called pores [28]. The strength of CPB is significantly affected by the cementing material. However, the kind, quantity, and transportation of the cementing material are limited by technical constraints and economic considerations [29,30]. The regulation of CPB pores mostly depends on the filling method.

The contact issue between the CPB and the goaf roof is evident [31]. Cemented paste backfill (CPB) is often used in engineering with mass ratios ranging from 1:2 to 1:12 of the cementing materials and particles. This refers to the percentage of particles in relation to the cementing ingredients. The CPB has a minimum of 66% according to reference [32]. Hence, it is essential to conduct a thorough examination of the impact of particles on the strength properties of CPB, with particular emphasis on the distribution of particle sizes [33]. Currently, the impact of particle size distribution on the strength of CPB varies significantly, leading to a lack of uniformity in the CPB material [34-37]. Nevertheless, there is a widespread belief that achieving the optimal strength characteristics of CPB relies on the appropriate particle size distribution [38-46]. Additionally, this distribution is thought to enhance the frost resistance and corrosion resistance of CPB [47] and even improve its flow property and water requirements [48].

II. THEORETICAL BACKGROUND

Governing Equation

$$k_t \frac{\partial e}{\partial t} - k \frac{\partial e}{\partial z} - Hcr \frac{\partial e}{\partial z} = \beta \dots\dots\dots (1)$$

Nomenclature

- Hcr = Compression Index, Void Ratio / PSD [L]
- Kt = Hydraulic Pressure/Specific Gravity [LT⁻¹]
- K = Permeability [LT⁻¹]

T = Time [T]
e = Uneven Settlement [-]
Z = Depth [L]

$$k_t \frac{\partial e}{\partial t} = k \frac{\partial e}{\partial z} - Hcr \frac{\partial e}{\partial z} + \beta \quad \dots\dots\dots (2)$$

$$k_t \frac{\partial e}{\partial t} = (k + Hcr) \frac{\partial e}{\partial z} + \beta \quad \dots\dots\dots (3)$$

$$k_t \frac{\partial e_1}{\partial t} = \beta \quad \dots\dots\dots (4)$$

$$\frac{\partial e_1}{\partial t} = \beta k_t \quad \dots\dots\dots (5)$$

$$e_1 = \beta k_t + \gamma \quad \dots\dots\dots (6)$$

$$k_t \frac{\partial e_1}{\partial t} = (k + Hcr) \frac{\partial e}{\partial z} \quad \dots\dots\dots (7)$$

Let $e_2 = ZT^1 \quad \dots\dots\dots (8)$

$$\frac{\partial e_2}{\partial t} = ZT^1 \quad \dots\dots\dots (9)$$

$$\frac{\partial e_2}{\partial z} = Z^1 T \quad \dots\dots\dots (10)$$

Substitute (9) and (10) into (7)

$$k_t ZT^1 = (k + Hcr) Z^1 T \quad \dots\dots\dots (11)$$

$$k_t \frac{T^1}{T} = (k + Hcr) \frac{Z^1}{Z} = \gamma \quad \dots\dots\dots (12)$$

$$k_t \frac{T^1}{T} = \gamma \quad \dots\dots\dots (13)$$

$$(k + Hcr) \frac{Z}{Z} = \gamma \quad \dots\dots\dots (14)$$

From (13), $\frac{T^1}{T} = \frac{\gamma}{k_t}$

$$\ln T = \frac{\gamma}{k_t} t + e_3 \quad \dots\dots\dots (15)$$

$$T = A e^{\frac{\gamma}{k_t} t} \quad \dots\dots\dots (16)$$

From (14), $(k + Hcr) \frac{Z}{Z} = \gamma$

$$\frac{Z}{Z} = \frac{\gamma}{k + Hcr} \quad \dots\dots\dots (17)$$

$$\ln Z = \frac{\gamma}{k + Hcr} Z + e_4 \quad \dots\dots\dots (18)$$

$$i.e. Z = \beta e^{\frac{\gamma}{k+Hcr} Z} \dots\dots\dots (19)$$

Putting (16) and (19) into (8) yields

$$e_2 = A e^{\frac{\gamma}{k_i} t} \cdot \beta e^{\frac{\gamma}{k+Hcr} Z} \dots\dots\dots (20)$$

$$e_2 = A \beta e^{\left(\frac{t}{k_i} + \frac{Z}{k+Hcr} \right) \gamma} \dots\dots\dots (21)$$

Hence, the general solution becomes

$$e(z, t) = e_1 + e_2$$

$$\left[e(z, t) = \beta k_i t + \gamma + A \beta e^{\left(\frac{t}{k_i} + \frac{Z}{k+Hcr} \right) \gamma} \right] \dots\dots\dots (22)$$

III. MATERIALS AND METHODS

Soil Sampling

Using an auger, we carefully collected undisturbed peat soil samples at various depths, specifically at intervals of 0.2 m, 0.4 m, 0.6 m, and so on, up to 2 m. Each sample was labelled and stored in sealed containers to prevent moisture loss, ensuring its integrity for laboratory analysis.

Geotechnical Analysis Moisture Content: we weighed the samples, dried them in an oven, and re-weighed them to calculate moisture content.

Density Measurement: we utilized Archimedes' principle to determine the density of the samples.

Shear Strength: By conducting triaxial tests, we assessed the shear strength characteristics, providing crucial insights into the load-bearing capacity of the peat soil.

Consolidation Tests: we used a consolidation apparatus to evaluate how the soil settled under applied loads over time, obtaining its compression index (Cc).

Monitoring Groundwater Levels we installed groundwater monitoring wells around the site to record fluctuations in water levels. These measurements were taken weekly to understand how changes in groundwater might influence the settling behaviour of the peat soil.

Instrumentation Setup: To monitor vertical displacements, we deployed settlement plates and rods at various key points throughout the site. we also conducted topographic surveys to establish baseline elevations. Regular surveys were scheduled to detect any elevation changes due to consolidation over time.

Load Application: To study the effect of weight on settlement, we imposed known loads on the top layer of the soil using strategically placed sandbags. This simulated real-world conditions where structures might be built atop the peat layers. We continuously recorded settlement data during this loading period.

Observation Duration: we ensured diligent monitoring over an extended period, collecting settlement readings at regular intervals—daily at first and then weekly as the process stabilized. After removing the loads, we continued to observe for any signs of recovery or further subsidence.

Data Collection and Analysis: After the observational period, we analyzed the data collected from the field instruments. we also correlated this field data with the laboratory test results to identify trends and relationships between soil composition, moisture content, and settlement characteristics. Using statistical methods, we developed a simulation

model to predict uneven settlement in peat soil based on the varying particle size distribution and compression index. We compared the model's predictions with my experimental data to validate its accuracy and sensitivity.

Reporting Results: Finally, we compiled all findings into a comprehensive report. we included detailed graphs displaying predicted versus experimental values over time and depth, highlighting the relationship between compressibility, particle size variability, and settlement. The report aimed to provide insights for engineering applications in peat environments and establish permissible limits for settlement in future construction projects.

Summary: This procedure not only enhanced my understanding of peat soil behaviour, but it also contributed valuable insights into managing settlement issues in geotechnical engineering. We emphasized the importance of ongoing research, advocating for continued data collection and model refinement to enhance prediction reliability in the context of peat soil dynamics.

IV. RESULTS AND DISCUSSION

Table 1: Predictive and Experimental Values of Uneven Settlement on Peat Soil

Depth [m]	Predictive Values of Uneven Settlement on Variation [PSD/Compression Index on Peat Soil [40/0.2] [mm]	Experimental Values of Uneven Settlement on Variation [PSD/Compression Index on Peat [40/0.2] [mm]
0.2	0.151895038	0.15192
0.4	0.152009324	0.15204
0.6	0.152123609	0.15216
0.8	0.152237895	0.15228
1	0.152352181	0.1524
1.2	0.152466467	0.15252
1.4	0.152580752	0.15264
1.6	0.152695038	0.15276
1.8	0.152809324	0.15288
2	0.15292361	0.153
2.2	0.153037895	0.15312
2.4	0.153152181	0.15324
2.6	0.153266467	0.15336
2.8	0.153380753	0.15348
3	0.153495038	0.1536
3.2	0.153609324	0.15372
3.4	0.15372361	0.15384
3.6	0.153837896	0.15396
3.8	0.153952182	0.15408
4	0.154066468	0.1542
4.2	0.154180754	0.15432
4.4	0.15429504	0.15444
4.6	0.154409326	0.15456
4.8	0.154523613	0.15468
5	0.154637899	0.1548

Volume 15, Issue 2, February 2026

|DOI: 10.15680/IJIRSET.2026.1502001|

5.2	0.154752186	0.15492
5.4	0.154866473	0.15504
5.6	0.154980761	0.15516
5.8	0.15509505	0.15528
6	0.155209339	0.1554
6.2	0.155323629	0.15552
6.4	0.15543792	0.15564
6.6	0.155552213	0.15576
6.8	0.155666509	0.15588
7	0.155780807	0.156
7.2	0.155895109	0.15612
7.4	0.156009415	0.15624
7.6	0.156123728	0.15636
7.8	0.156238049	0.15648
8	0.15635238	0.1566
8.2	0.156466724	0.15672
8.4	0.156581086	0.15684
8.6	0.156695471	0.15696
8.8	0.156809884	0.15708
9	0.156924336	0.1572
9.2	0.157038836	0.15732
9.4	0.1571534	0.15744
9.6	0.157268046	0.15756
9.8	0.157382799	0.15768
10	0.157497689	0.1578
10.2	0.157612759	0.15792
10.4	0.15772806	0.15804
10.6	0.157843662	0.15816
10.8	0.157959652	0.15828
11	0.158076146	0.1584
11.2	0.158193294	0.15852
11.4	0.158311287	0.15864
11.6	0.158430377	0.15876
11.8	0.158550887	0.15888
12	0.158673237	0.159
12.2	0.15879797	0.15912
12.4	0.158925793	0.15924
12.6	0.159057618	0.15936
12.8	0.159194627	0.15948
13	0.159338355	0.1596
13.2	0.159490787	0.15972

13.4	0.159654496	0.15984
13.6	0.159832816	0.15996
14	0.160251846	0.1602
14.2	0.160505403	0.16032

Table 2: Predictive and Experimental Values of Uneven Settlement on Peat Soil

Time	Predictive Values Settlement of Uneven Variation [PSD/Compression Index on Peat Soil [42/0.223] [mm]	Experimental Values of Uneven Settlement on Variation [PSD/Compression Index on Peat soil [42/0.223] [mm]
0.02	0.223009964	0.213762167
0.04	0.223017965	0.214216698
0.05	0.223021966	0.214441113
0.07	0.223029967	0.214884269
0.08	0.223033967	0.215103021
0.085	0.223035967	0.215211693
0.09	0.223037967	0.215319896
0.095	0.223039968	0.215427632
0.1	0.223041968	0.2155349
0.15	0.22306197	0.216582038
0.2	0.223009964	0.213762167
0.25	0.223101974	0.218539063
0.3	0.223121976	0.2194503
0.35	0.223141978	0.220317588
0.4	0.22316198	0.2211416
0.45	0.223181983	0.221923013
0.5	0.223201985	0.2226625
0.55	0.223221987	0.223360738
0.6	0.223241989	0.2240184
0.65	0.223261992	0.224636163
0.7	0.223281994	0.2252147
0.75	0.223301996	0.225754688
0.8	0.223321999	0.2262568
0.85	0.223342001	0.226721713
0.9	0.223362003	0.2271501
0.95	0.223382006	0.227542638
1	0.223402008	0.2279
1.25	0.223502022	0.229182813
1.5	0.223602039	0.2296875

2	0.223802089	0.2287
2.25	0.223902133	0.227376563
2.5	0.224002199	0.2256125
2.75	0.224102306	0.223492188
3	0.224202482	0.2211
3.25	0.224302777	0.218520313
3.5	0.224403273	0.2158375
3.75	0.224504116	0.213135938
4	0.224605553	0.2105
4.25	0.224708004	0.208014063
4.5	0.224812195	0.2057625
4.75	0.224919361	0.203829688
5.25	0.225152605	0.201257813
5.5	0.225288521	0.2007875
5.75	0.225449999	0.200973438
6	0.22565524	0.2019
6.25	0.2259354	0.203651563
6.5	0.226343818	0.2063125
6.75	0.226971809	0.209967188
7	0.227975697	0.2147
7.25	0.229623102	0.220595313
7.5	0.232372179	0.2277375
7.75	0.237007265	0.236210938
8	0.244871109	0.2461
8.25	0.258262432	0.257489063
9	0.386957737	0.3015

Table 3: Predictive and Experimental Values of Uneven Settlement on Peat Soil

Depth [m]	Predictive Values of Uneven Settlement on Variation [PSD/Compression Index on Peat soil [30/0.21] [mm]	Experimental Values of Uneven Settlement on Variation [PSD/Compression Index on Peat Soil [mm]
0.2	0.370749618	0.35624216
0.4	0.370751156	0.35947728
0.6	0.370752695	0.36241832
0.8	0.370754233	0.36507824
1	0.370755772	0.36747
1.2	0.37075731	0.36960656
1.4	0.370758848	0.37150088

Volume 15, Issue 2, February 2026

|DOI: 10.15680/IJIRSET.2026.1502001|

1.6	0.370760387	0.37316592
1.8	0.370761925	0.37461464
2	0.370763464	0.37586
2.2	0.370765002	0.37691496
2.4	0.370766541	0.37779248
2.6	0.370768079	0.37850552
2.8	0.370769618	0.37906704
3	0.370771156	0.37949
3.2	0.370772695	0.37978736
3.4	0.370774233	0.37997208
3.6	0.370775772	0.38005712
3.8	0.37077731	0.38005544
4	0.370778849	0.37998
4.2	0.370780387	0.37984376
4.4	0.370781926	0.37965968
4.6	0.370783464	0.37944072
4.8	0.370785003	0.37919984
5	0.370786542	0.37895
5.2	0.370788081	0.37870416
5.4	0.37078962	0.37847528
5.6	0.370791159	0.37827632
5.8	0.370792699	0.37812024
6	0.37079424	0.37802
6.2	0.370795783	0.37798856
6.4	0.370797327	0.37803888
6.6	0.370798874	0.37818392
6.8	0.370800425	0.37843664
7	0.370801983	0.37881
7.2	0.370803552	0.37931696
7.4	0.370805135	0.37997048
7.6	0.370806741	0.38078352
7.8	0.370808382	0.38176904
8	0.370810076	0.38294
8.2	0.37081185	0.38430936
8.4	0.370813743	0.38589008
8.6	0.370815819	0.38769512
8.8	0.37081817	0.38973744
9	0.370820937	0.39203
9.2	0.370824333	0.39458576
9.4	0.37082868	0.39741768
9.6	0.370834467	0.40053872

9.8	0.370842429	0.40396184
10	0.370853682	0.4077
10.2	0.37086991	0.41176616
10.4	0.370893662	0.41617328
10.6	0.370928791	0.42093432
10.8	0.370981126	0.42606224
11	0.37105948	0.43157
11.2	0.371177177	0.43747056
11.4	0.371354371	0.44377688
11.6	0.371621536	0.45050192
11.8	0.372024755	0.45765864
12	0.372633713	0.46526
12.2	0.373553791	0.47331896
12.4	0.374944345	0.48184848
12.6	0.377046351	0.49086152
12.8	0.380224215	0.50037104
13	0.385028989	0.51039
13.2	0.392293977	0.52093136
13.4	0.403279296	0.53200808
13.6	0.419890497	0.54363312
14	0.482992772	0.56858
14.2	0.540430778	0.58192776

Table 4: Predictive and Experimental Values of Uneven Settlement on Peat Soil

Time of Settlement	Predictive Values of Uneven Settlement on Variation [PSD/Compression Index on Peat Soil [mm]]	Experimental Values of Uneven Settlement on Variation [PSD/Compression Index on Peat Soil [mm]]
0.02	0.26001096	0.259528683
0.04	0.26001976	0.259061706
0.06	0.26002856	0.258609811
0.075	0.26003516	0.258280655
0.08	0.26003736	0.258172778
0.085	0.26003956	0.258065817
0.09	0.26004176	0.257959768
0.095	0.26004396	0.257854628
0.1	0.26004616	0.257750393
0.15	0.26006816	0.256757102
0.02	0.26001096	0.259528683

Volume 15, Issue 2, February 2026

|DOI: 10.15680/IJIRSET.2026.1502001|

0.25	0.26011216	0.255027874
0.3	0.26013416	0.254285433
0.35	0.26015616	0.253620187
0.4	0.260178161	0.253029008
0.45	0.260200161	0.252508817
0.5	0.260222161	0.252056585
0.55	0.260244161	0.251669332
0.6	0.260266162	0.251344128
0.65	0.260288162	0.251078092
0.7	0.260310162	0.250868393
0.75	0.260332163	0.250712249
0.8	0.260354163	0.250606928
0.85	0.260376164	0.250549747
0.9	0.260398164	0.250538073
0.95	0.260420165	0.250569322
1	0.260442165	0.25064096
1.25	0.26055217	0.251519749
1.5	0.260662178	0.253056585
2	0.260882215	0.25709096
2.25	0.260992255	0.259159124
2.5	0.261102323	0.261026585
2.75	0.26121244	0.262555999
3	0.26132264	0.26364096
3.25	0.261432982	0.264205999
3.5	0.261543568	0.264206585
3.75	0.261654572	0.263629124
4	0.26176629	0.26249096
4.25	0.261879232	0.260840374
4.5	0.261994267	0.258756585
4.75	0.262112888	0.256349749
5.25	0.262372912	0.251162249
5.5	0.262526165	0.248756585
5.75	0.262710212	0.246777874
6	0.262946977	0.24549096
6.25	0.263273994	0.245191624
6.5	0.263755515	0.246206585
6.75	0.264501543	0.248893499
7	0.265700391	0.25364096
7.25	0.267674448	0.260868499
7.5	0.270975623	0.271026585
7.75	0.276548764	0.284596624

8	0.2860114	0.30209096
8.25	0.302132666	0.324052874
9	0.457132935	0.42264096

Table 5: Predictive and Experimental Values of Uneven Settlement on Peat Soil

Time of Settlement	Predictive Values of Uneven Settlement on Variation [PSD/Compression Index on Peat Soil [44/0.24] [mm]	Experimental Values of Uneven Settlement on Variation [PSD/Compression Index on Peat Soil [44/0.24] [mm]
0.02	0.24001096	0.233482008
0.04	0.24001976	0.233956064
0.05	0.24002416	0.234190125
0.07	0.24003296	0.234652343
0.08	0.24003736	0.234880512
0.085	0.24003956	0.234993864
0.09	0.24004176	0.235106729
0.095	0.24004396	0.235219107
0.1	0.24004616	0.235331
0.15	0.24006816	0.236423375
0.2	0.24001096	0.233482008
0.25	0.24011216	0.238465625
0.3	0.24013416	0.239417
0.35	0.24015616	0.240322875
0.4	0.240178161	0.241184
0.45	0.240200161	0.242001125
0.5	0.240222161	0.242775
0.55	0.240244161	0.243506375
0.6	0.240266161	0.244196
0.65	0.240288162	0.244844625
0.7	0.240310162	0.245453
0.75	0.240332162	0.246021875
0.8	0.240354163	0.246552
0.85	0.240376163	0.247044125
0.9	0.240398164	0.247499
0.95	0.240420164	0.247917375
1	0.240442165	0.2483
1.25	0.240552169	0.249703125
1.5	0.240662177	0.250325
2	0.240882212	0.2496

Volume 15, Issue 2, February 2026**|DOI: 10.15680/IJRSET.2026.1502001|**

2.25	0.24099225	0.248440625
2.5	0.241102316	0.246875
2.75	0.241212428	0.244996875
3	0.241322619	0.2429
3.25	0.241432946	0.240678125
3.5	0.241543507	0.238425
3.75	0.241654467	0.236234375
4	0.241766111	0.2342
4.25	0.241878924	0.232415625
4.5	0.241993741	0.230975
4.75	0.242111987	0.229971875
5.25	0.24237027	0.229653125
5.5	0.242521643	0.230525
5.75	0.242702471	0.232209375
6	0.242933724	0.2348
6.25	0.243251305	0.238390625
6.5	0.243716674	0.243075
6.75	0.244435048	0.248946875
7	0.245586555	0.2561
7.25	0.247479565	0.264628125
7.5	0.250641994	0.274625
7.75	0.255977607	0.286184375
8	0.265033607	0.2994
8.25	0.280458731	0.314365625
9	0.428734206	0.3707

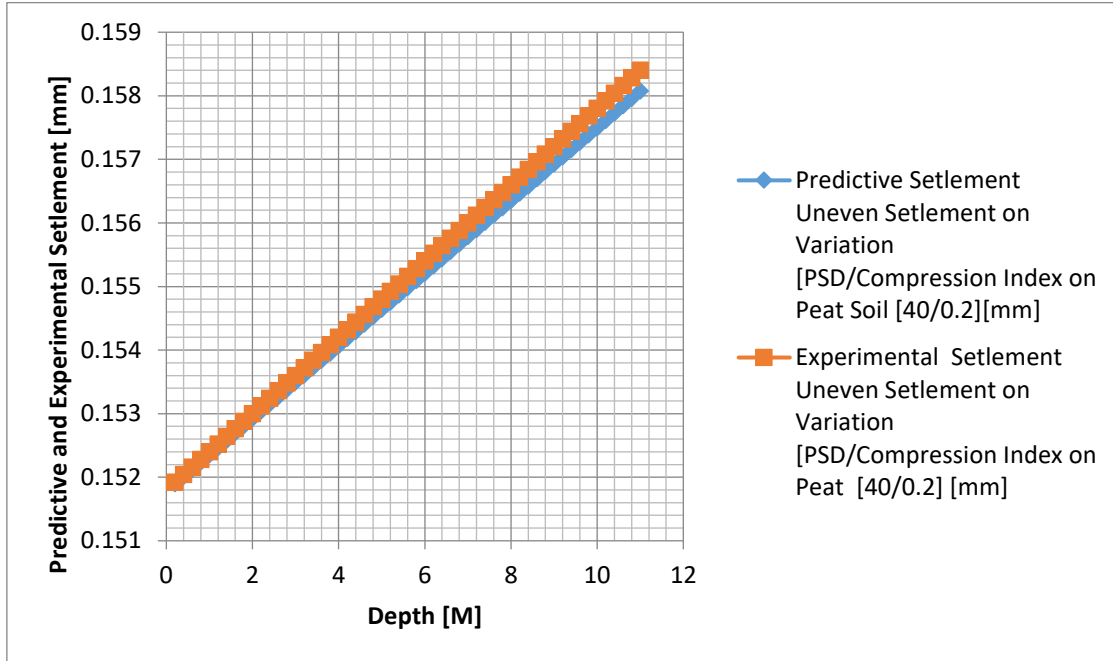


Figure 1: Predictive and Experimental Values of Uneven Settlement on Peat Soil

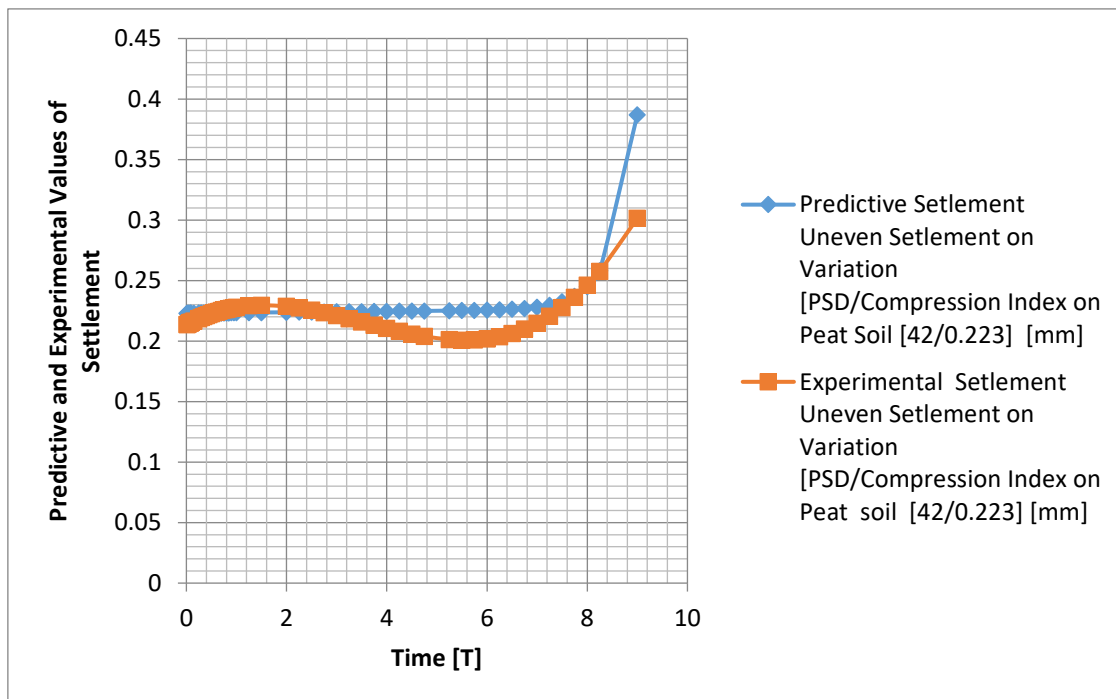


Figure 2: Predictive and Experimental Values of Uneven Settlement on Peat Soil

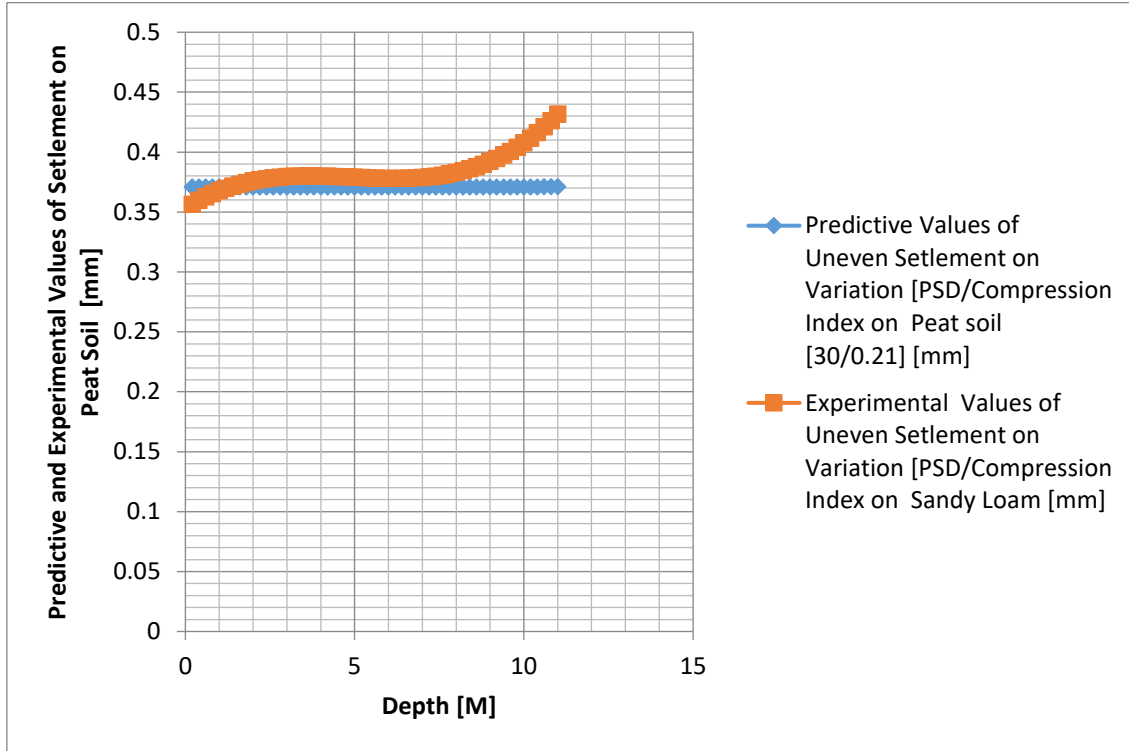


Figure 3: Predictive and Experimental Values of Uneven Settlement on Peat Soil

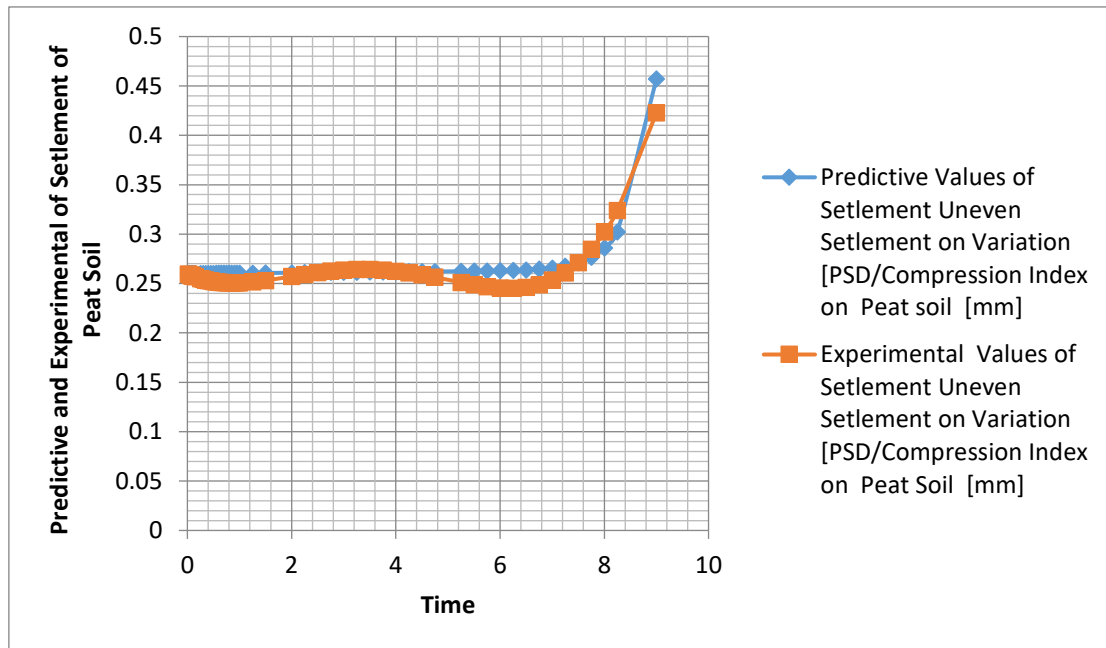


Figure 4: Predictive and Experimental Values of Uneven Settlement on Peat Soil

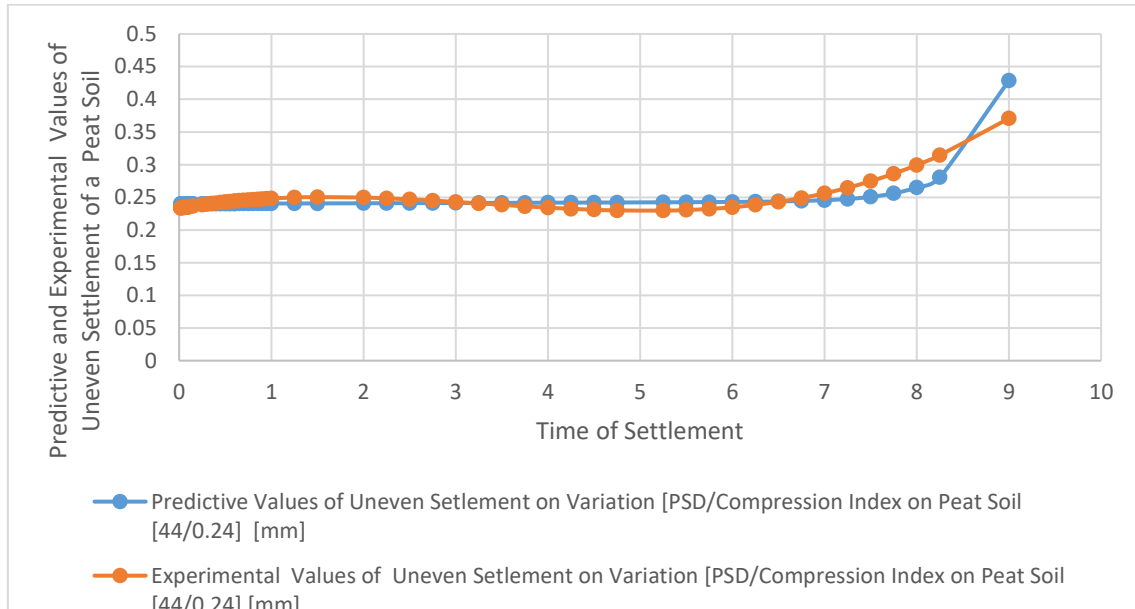


Figure 5: Predictive and Experimental Values of Uneven Settlement on Peat Soil

Heterogeneous Particle Size Distribution: Peat soil consists of organic materials and has a significant water content. It often comprises a diverse assortment of particle sizes, including fibres, roots, and decomposed plant matter. Heterogeneous particle size distribution in soil indicates the presence of particles of different sizes distributed uniformly across its whole. Peat soil with a varied range of particle sizes might experience uneven settling as a result of the differential compression of these distinct particle sizes. Smaller particles, such as small fibres and organic materials, exhibit greater compressibility compared to bigger particles, such as roots or woody debris. Consequently, while consolidating, the smaller particles may compress more quickly and to a bigger degree than the larger ones. The differential compression results in uneven settlement, with regions with a greater concentration of smaller particles experiencing more settling compared to regions with bigger particles. Differential ground movements caused by non-uniform settlement may lead to unevenness and possible structural issues in structures or infrastructure built on peat soil. The compression index, often known as C_c , is a geotechnical measure used to quantify the compressibility of a soil. The consolidation coefficient is obtained via consolidation tests and corresponds to the gradient of the compression curve when plotted on a semilogarithmic scale. The compression index is a measure of the extent to which a soil consolidates in response to a certain increase in effective stress. The compression index in peat soil indicates the degree of compressibility of the organic matter found within it. A higher compression index signifies more compressibility, indicating that the soil experiences more settlement in response to a given increase in stress. Peat soil with a high compression index is prone to experiencing substantial settling during the consolidation process. The settlement might worsen if there are spatial variations in the compression index within the soil mass. Regions with higher compression index values will undergo more settlement in comparison to regions with lower compression index values.

Hence, peat soil with a substantial compression index will result in disparate settling, since distinct regions of the soil will undergo varying degrees of compression. Such uneven compression might lead to differential settling and possible structural problems. To finally the uneven settling of peat soil is influenced by both the heterogeneous particle size distribution and the compression index. Differential compression occurs due to the existence of particles of varying sizes, resulting in greater settling of smaller particles compared to bigger ones. Furthermore, a high compression index signifies a greater degree of compressibility and an elevated likelihood of settlement. Hence, the amalgamation of various elements may result in disparate settlement patterns in peat soil. In order to verify the accuracy of the created simulation model for uneven settlement in peat soil, two distinct types of graphs can be employed. The first graph plots the predicted simulation values on the y-axis against the z-axis, which represents time. The second graph plots the predicted simulation values on the y-axis against the x-axis, which represents the depth of settlement. Graph depicting the predicted simulation values on the y-axis plotted against the z-axis (representing time). The y-axis in this graph

reflects the forecasted simulation values of settlement, while the z-axis represents time. Each data point on the graph represents a distinct moment in the settlement process, and the settlement values are shown appropriately. Through an analysis of this graph, one may discern the fluctuations in settlement values over time as dictated by the simulation model. The graph should ideally demonstrate a distinct trend or pattern that aligns with the anticipated behaviour of settling in peat soil. The simulation model must precisely depict the chronological development of settlement, including any temporal fluctuations or phases in the settlement process.

A strong correlation between the predictive simulation results and the z-axis (time) suggests that the model accurately reproduces the time-dependent settlement behaviour in peat soil. Any inconsistencies or divergences between the projected values and the anticipated pattern may indicate potential areas for improvement in the simulation model. Graph depicting the predicted simulation values on the y-axis in relation to the x-axis, which represents the depth of settlement. The y-axis of this graph displays the anticipated simulation values of settlement, while the x-axis represents the depth inside the peat soil where settlement is measured. Every data point on the graph represents a distinct depth, and the settlement values are represented correspondingly. This graph enables you to analyse the depth-dependent behaviour of settlement as projected by the simulation model. It aids in evaluating the model's ability to accurately represent fluctuations in settlement rates at various depths inside the peat soil. The graph demonstrates a consistent trend or pattern that corresponds to the predictive behaviour of settlement in relation to depth. An accurate correspondence between the predictive simulation values and the x-axis (depth) suggests that the model effectively replicates the depth-dependent fluctuations in settlement. If the model accurately predicts the settlement patterns at various depths, it indicates that the model is capable of capturing the spatial distribution of settlement in peat soil. By examining these graphs depicting simulated values against the z-axis (representing time) and the x-axis (representing settlement depth), one may verify the simulation model's capacity to accurately reproduce the temporal and spatial fluctuations in uneven settlement. A high correlation and excellent alignment between the projected values and the anticipated trends suggest a dependable and proven model. Any inconsistencies or deviations seen on the graphs might provide valuable insights for conducting more research and making enhancements to the model, hence improving its accuracy and dependability in forecasting uneven settling in peat soil.

V. CONCLUSION

To summarize, the discussion was on the application of graphs to verify a simulation model for non-uniform subsidence in peat soil. Two kinds of graphs were analysed: one displaying expected simulation values on the y-axis against the z-axis (representing time), and another displaying anticipated simulation values on the y-axis against the x-axis (representing depth of settlement). When examining the graph that displays projected values over time, it is crucial to analyse the pattern, detect any delays in time, and evaluate how the model's performance is affected by time parameters. The graph should demonstrate patterns that correspond to the anticipated settlement behaviour over time, suggesting that the model effectively captures the temporal features of settlement. The primary objective of analyzing the graph depicting anticipated values versus depth is to assess the settlement's behaviour as it varies with depth. The study includes the examination of depth profiles, the comparison of the findings with field data, and the evaluation of the model's sensitivity to depth parameters. The graph should illustrate the model's precise depiction of the spatial arrangement of settlements at various depths inside the peat soil. By implementing these study suggestions, the simulation model for uneven settlement in peat soil may be further verified, improved, and augmented, resulting in a more dependable tool for forecasting settlement behavior in real-life situations.

REFERENCES

1. Khoshand, A.; Fall, M. Geotechnical characterization of peat-based landfill cover materials. *J. Rock Mech. Geotech. Eng.* 2016, 6, 1–9. [CrossRef]
2. Deng, D.Q.; Liu, L.; Yao, Z.L.; Song, K.; Lao, D.Z. A practice of ultra-fine tailings disposal as filling material in a gold mine. *J. Environ. Manag.* 2017, 196, 100–109. [CrossRef] [PubMed]
3. Li, M.; Zhang, J.X.; Zhou, N.; Huang, Y.L. Effect of Particle Size on the Energy Evolution of Crushed Waste Rock in Coal Mines. *Rock Mech. Rock Eng.* 2017, 50, 1–8. [CrossRef]
4. Li, X.B.; Li, D.Y.; Liu, Z.X.; Zhao, G.Y.; Wang, W.H. Determination of the minimum thickness of crown pillar for safe exploitation of a subsea gold mine based on numerical modelling. *Int. J. Rock Mech. Min. Sci.* 2013, 57, 42–56. [CrossRef]

5. Zhang, J.X.; Li, B.Y.; Zhou, N.; Zhang, Q. Application of solid backfilling to reduce hard-roof caving and longwall coal face burst potential. *Int. J. Rock Mech. Min. Sci.* 2016, 88, 197–205. [CrossRef]
6. Zhang, K.; Yang, T.H.; Bai, H.B.; Gamage, R.P. Longwall mining-induced damage and fractures: Field measurements and simulation using FDM and DEM coupled method. *Int. J. Geomech.* 2018, 18, 04017127. [CrossRef]
7. Sivakugan, N.; Rankine, R.M.; Rankine, K.J.; Rankine, K.S. Geotechnical considerations in mine backfilling in Australia. *J. Clean. Prod.* 2006, 14, 1168–1175. [CrossRef]
8. Abdul-Hussain, N.; Fall, M. Thermo-hydro-mechanical behaviour of sodium silicate-cemented paste tailings in column experiments. *Tunn. Undergr. Space Technol.* 2012, 29, 85–93. [CrossRef]
9. Holt, E.; Leivo, M. Cracking risks associated with early age shrinkage. *Cem. Concr. Compos.* 2004, 26, 521–530. [CrossRef]
10. Ouellet, S.; Bussière, B.; Aubertin, M.; Benzaazoua, M. Characterization of cemented paste backfill pore structure using SEM and IA analysis. *Bull. Eng. Geol. Environ.* 2008, 67, 139–152. [CrossRef]
11. Wu, A.X.; Wang, Y.; Wang, H.J.; Yin, S.H.; Miao, X.X. Coupled effects of cement type and water quality on the properties of cemented paste backfill. *Int. J. Min. Process.* 2015, 143, 65–71. [CrossRef]
12. Ouellet, S.; Bussière, B.; Mbonimpa, M.; Benzaazoua, M.; Aubertin, M. Reactivity and mineralogical evolution of an underground mine sulphidic cemented paste backfill. *Miner. Eng.* 2006, 19, 407–419. [CrossRef]
13. Fall, M.; Benzaazoua, M.; Saa, E.G. Mix proportioning of underground cemented tailings backfill. *Tunn. Undergr. Space Technol.* 2008, 23, 80–90. [CrossRef]
14. Koohestani, B.; Koubaa, A.; Belem, T.; Bussière, B.; Bouzazhah, H. Experimental investigation of mechanical and microstructural properties of cemented paste backfill containing maple-wood filler. *Constr. Build. Mater.* 2016, 121, 222–228. [CrossRef]
15. Ercikdi, B.; Cihangir, F.; Kesimal, A.; Deveci, H.; Alp, I. Utilization of water-reducing admixtures in cemented paste backfill of sulphide-rich mill tailings. *J. Hazard. Mater.* 2010, 179, 940–946. [CrossRef] [PubMed]
16. Koohestani, B.; Darban, A.K.; Mokhtari, P. A comparison between the influence of superplasticizer and organosilanes on different properties of cemented paste backfill. *Constr. Build. Mater.* 2018, 173, 180–188. [CrossRef]
17. Koohestani, B.; Bussière, B.; Belem, T.; Koubaa, A. Influence of polymer powder on properties of cemented paste backfill. *Int. J. Min. Process.* 2017, 167, 1–8. [CrossRef]
18. Koohestani, B. Effect of saline admixtures on mechanical and microstructural properties of cementitious matrices containing tailings. *Constr. Build. Mater.* 2017, 156, 1019–1027. [CrossRef]
19. Pourjavadi, A.; Fakoorpoor, S.M.; Hosseini, P.; Khaloo, A. Interactions between superabsorbent polymers and cement-based composites incorporating colloidal silica nanoparticles. *Cem. Concr. Compos.* 2013, 37, 196–204. [CrossRef]
20. Koohestani, B.; Belem, T.; Koubaa, A.; Bussière, B. Experimental investigation into the compressive strength development of cemented paste backfill containing Nano-silica. *Cem. Concr. Compos.* 2016, 72, 180–189. [CrossRef]
21. Fall, M.; Célestin, J.C.; Pokharel, M.; Touré, M. A contribution to understanding the effects of curing temperature on the mechanical properties of mine cemented tailings backfill. *Eng. Geol.* 2010, 114, 397–413. [CrossRef]
22. Fall, M.; Pokharel, M. Coupled effects of sulphate and temperature on the strength development of cemented tailings backfills: Portland cement-paste backfill. *Cem. Concr. Compos.* 2010, 32, 819–828. [CrossRef]
23. Fall, M.; Samb, S.S. Effect of high temperature on strength and microstructural properties of cemented paste backfill. *Fire Saf. J.* 2009, 44, 642–651. [CrossRef]
24. Ghirian, A.; Fall, M. Coupled thermo-hydro-mechanical-chemical behaviour of cemented paste backfill in column experiments. Part II: Physical, hydraulic and thermal processes and characteristics. *Eng. Geol.* 2013, 164, 195–207. [CrossRef]
25. Jiang, H.; Fall, M.; Liang, C. Yield stress of cemented paste backfill in sub-zero environments: Experimental results. *Miner. Eng.* 2016, 92, 141–150.
26. Yilmaz, E.; Belem, T.; Benzaazoua, M. Effects of curing and stress conditions on hydromechanical, geotechnical and geochemical properties of cemented paste backfill. *Eng. Geol.* 2014, 168, 23–37. [CrossRef]
27. Cihangir, F.; Ercikdi, B.; Kesimal, A.; Deveci, H.; Erdemir, F. Paste backfill of high-sulphide mill tailings using alkali-activated blast furnace slag: Effect of activator nature, concentration and slag properties. *Miner. Eng.* 2015, 83, 117–127. [CrossRef]
28. Jongpradist, P. Effective Void Ratio for Assessing the Mechanical Properties of Cement-Clay Admixtures at High Water Content. *J. Geotech. Geoenviron.* 2011, 137, 621–627. [CrossRef]
29. Yilmaz, E.; Benzaazoua, M.; Belem, T.; Bussière, B. Effect of curing under pressure on compressive strength development of cemented paste backfill. *Miner. Eng.* 2009, 22, 772–785. [CrossRef]

30. Liu, Z.X.; Dang, W.G.; Liu, Q.L.; Chen, G.H.; Peng, K. Optimization of clay material mixture ratio and filling process in gypsum mine goaf. *Int. J. Min. Sci. Technol.* 2013, 23, 337–342. [CrossRef]
31. Miao, X.X.; Zhang, J.X.; Feng, M.M. Waste-filling in fully-mechanized coal mining and its application. *J. China Univ. Min. Technol.* 2008, 18, 479–482. [CrossRef]
32. Liu, Z.X.; Li, X.B. Study on fractal gradation of tailings and knowledge bank of its cementing strength. *Chin. J. Rock Mech. Eng.* 2005, 24, 1789–1793.
33. Yin, S.H.; Wu, A.X.; Hu, K.J.; Wang, Y.; Zhang, Y.K. The effect of solid components on the rheological and mechanical properties of cemented paste backfill. *Miner. Eng.* 2012, 35, 61–66. [CrossRef]
34. Ke, X.; Hou, H.; Zhou, M.; Wang, Y.; Zhou, X. Effect of particle gradation on properties of fresh and hardened cemented paste backfill. *Constr. Build. Mater.* 2015, 96, 378–382. [CrossRef]
35. Fall, M.; Benzaazoua, M.; Ouellet, S. Experimental characterization of the influence of tailings fineness and density on the quality of cemented paste backfill. *Miner. Eng.* 2005, 18, 41–44. [CrossRef]
36. Börjesson, L.; Johannesson, L.E.; Gunnarsson, D. Influence of soil structure heterogeneities on the behaviour of backfill materials based on mixtures of bentonite and crushed rock. *Appl. Clay Sci.* 2003, 23, 121–131. [CrossRef]
37. Yilmaz, E.; Belem, T.; Benzaazoua, M.; Kesimal, A.; Ercikdi, B. Evaluation of the strength properties of deslimed tailings paste backfill. *Miner. Resour. Eng.* 2013, 12, 129–144.
38. Orejarena, L.; Fall, M. The use of artificial neural networks to predict the effect of sulphate attack on the strength of cemented paste backfill. *Bull. Eng. Geol. Environ.* 2010, 69, 659–670. [CrossRef]
39. Gautam, B.P.; Panesar, D.K.; Sheikh, S.A.; Vecchio, F.J. Effect of coarse aggregate grading on the ASR expansion and damage of concrete. *Cem. Concr. Res.* 2017, 95, 75–83. [CrossRef]
40. Liu, R.; Li, B.; Jiang, Y. Critical hydraulic gradient for nonlinear flow through rock fracture networks: The roles of aperture, surface roughness, and number of intersections. *Adv. Water. Resour.* 2016, 88, 53–65. [CrossRef]
41. Liu, R.; Jiang, Y.; Li, B.; Yu, L. Estimating permeability of porous media based on modified Hagen–Poiseuille flow in tortuous capillaries with variable lengths. *Microfluid. Nanofluid.* 2016, 20, 120. [CrossRef]
42. Yilmaz, E.; Benzaazoua, M.; Bussière, B.; Kesimal, A.; Ercikdi, B. Influence of disposal configurations on hydrogeological behaviour of sulphidic paste tailings: A field experimental study. *Int. J. Miner. Process.* 2014, 131, 12–25. [CrossRef]
43. Ke, X.; Zhou, X.; Wang, X.; Wang, T.; Hou, H.B.; Zhou, M. Effect of tailings fineness on the pore structure development of cemented paste backfill. *Constr. Build. Mater.* 2016, 126, 345–350. [CrossRef]
44. Kesimal, A.; Ercikdi, B.; Yilmaz, E. The effect of desliming by sedimentation on paste backfill performance. *Miner. Eng.* 2003, 16, 1009–1011. [CrossRef]
45. Sari, D.; Pasamehmetoglu, A.G. The effects of gradation and admixture on the pumice lightweight aggregate concrete. *Cem. Concr. Res.* 2005, 35, 936–942. [CrossRef]
46. Bosiljkov, V.B. SCC mixes with poorly graded aggregate and high volume of limestone filler. *Cem. Concr. Res.* 2003, 33, 1279–1286. [CrossRef]
47. Lamontagne, A.; Pigeon, M. The influence of polypropylene fibers and aggregate grading on the properties of dry-mix shotcrete. *Cem. Concr. Res.* 1995, 25, 293–298. [CrossRef]
48. Zhang, T.S.; Yu, Q.J.; Wei, J.X.; Zhang, P.P. A new gap-graded particle size distribution and resulting consequences on properties of blended cement. *Cem. Concr. Compos.* 2011, 33, 543–550. [CrossRef]
- [49] Jiangyu W, Meimei F Zhanqing C Xianbiao M Guansheng Han and Yiming W. Particle Size Distribution Effects on the Strength Characteristic of Cemented Paste Backfill [MDPI] *Minerals* 2018, 8, 322; doi:10.3390/min8080322



INTERNATIONAL
STANDARD
SERIAL
NUMBER
INDIA



INTERNATIONAL JOURNAL OF INNOVATIVE RESEARCH

IN SCIENCE | ENGINEERING | TECHNOLOGY

 9940 572 462  6381 907 438  ijirset@gmail.com



www.ijirset.com

Scan to save the contact details